Characterization and Crack Propagation Behavior of $ZrO_2-Al_2O_3$ Composites with High Fracture Strength

Ryoichi Shikata*, Yoshinori Urata*,
Takeshi Shiono** and Tomozo Nishikawa**

* Advanced Materials Research Laboratory, Osaka Cement Co.Ltd., Minamiokajima, Taisho-ku, Osaka 551, Japan

** Faculty of Engineering and Design, Kyoto Institute of Technology, Goshokaido-cho, Matsugasaki, Sakyo-ku, Kyoto 606, Japan

Abstract

ZrO_2-Al_2O_3 composites with high fracture strength were developed. The maximum bending strength occured at Al_2O_3 content from 20 to 40 wt% and reached about 3000 MPa. Fracture toughness measured by SEPB method showed the same trend as bending strength and was found maximum as high as about 7.5 $MPam^{1/2}$. And then, each of large Al_2O_3 grains was dispersed in the matrix of ZrO_2 with small grains.

The addition of Al_2O_3 reduced the grain size of tetragonal ZrO_2 and caused the residual stresses due to the thermal expansion mismatch between ZrO_2 and Al_2O_3. Compressive stress in ZrO_2 grains and tensile stress in Al_2O_3 grains were observed. These residual stresses led to the strengthening of Al_2O_3 grains and the fracture mode change from inter-granular to trans-granular fracture at ZrO_2 grains. Consequently, it was concluded that the enhancement of fracture strength resulted in the increase in fracture toughness, the rise of critical stress to initiate tetragonal to

monoclinic ZrO_2 transformation and the reduction of flaw size as fracture origins.

1. Introduction

Tetragonal zirconia polycrystals (TZP) attract now much attention as a structural ceramics because of high fracture strength and toughness. It was reported that the mechanism of TZP to develop such high fracture strength and toughness was its martensitic stress-induced phase transformation[1]. It has, however, some disadvantages such as decrease in fracture strength at higher temperatures, low hardness and degradation due to aging at about 100 to 300℃, which are now the obstacles in the development of its applications. For its wide use in future, fracture strength, toughness and reliability of TZP should be enhanced further in addition to the improvement of the disadvantages mentioned above. To meet these diversified needs, however, monolithic zirconia ceramics have a limitation. Consequently, composites of ZrO_2 and other suitable ceramics have recently attracted much attention[2)-7)].

By the optimum selection of preparation conditions such as starting raw materials, pre-sintering and isostatic hot-pressing, the authors succeeded recently to develop ZrO_2-Al_2O_3 composites that have average bending strength as high as about 3000 MPa[8]. In the present work, to make clear the mechanism that gave the ZrO_2-Al_2O_3 composites high fracture strength and toughness, the effects of microstructures and residual stresses were investigated.

2. Experimental procedure

Two kinds of zirconia powder containing Y_2O_3 of 2 and 3 mol% respectively were prepared by hydrolysis method. Table I showed characteristics of raw zirconia powders. These raw zirconia powders were mixed homogeneously with high purity alumina powder shown in Table II. The homogeneously mixed powders were mold-pressed at 39 MPa, and then isostatically cold-pressed at 98 MPa. To obtain densely sintered bodies, the green compacts were pre-sintered for 3 hours with changing temperature depending on the Al_2O_3 content: at 1400℃ for 0 to 20 wt% Al_2O_3 content, at 1500℃ for 40 wt% Al_2O_3 content, and at 1600℃ for 60 to 100 wt% Al_2O_3 content. The pre-sintered bodies were further isostatically hot-pressed under argon atmosphere for 1 hour at 1450℃ and 98 MPa, resulting finally in plates with diameter of about 50 mm and thickness of about 3.5 mm[8).

From each plates, test specimens were prepared according to JIS R 160 1, and were used in all of the following tests. Three-point-bending strength was measured according to JIS R 1601. Fracture toughness was measured according to single-edge-precracked-beam (SEPB) method specified in JIS R 1607. Crack propagation behaviors by a Vickers indenter were observed by scanning electron microscopy (SEM: HITACHI s-800).

Microstructure was analyzed by SEM (HITACHI s-800). From this analysis, mean grain sizes of ZrO_2 and Al_2O_3 were measured by intercept method. In addition, monoclinic and cubic phase contents of ZrO_2 were calculated by X-ray diffraction method[9).

Residual stresses of the composites were measured by X-ray diffraction method. A parallel-beam slits and an incident angle setting mechanism for iso-inclination method were attached to X-ray diffractometers (SHIMAZU XD-3A, 610). The phase stresses of ZrO_2 and Al_2O_3 in the composites were measured according to the conditions shown in Table III. Furthermore, macrostresses and microstresses were calculated from these phase stresses and volume fractions[10].

3. Results and Discussion

(1) Bending strength

The addition of Al_2O_3 to ZrO_2 was remarkably effective for the enhancement of fracture strength. Fig. 1 shows the bending streength of ZrO_2-Al_2O_3 composites as a function of Al_2O_3 content. With regard to Y_2O_3 content, 2 and 3 mol% composites showed nealy the same tendency. With regard to Al_2O_3 content, in both systems, average bending strength was found as high as about 3000 MPa for the composites from 20 to 40 wt% Al_2O_3.

(2) Fracture toughness

Similarly, Fig. 2 shows fracture toughness as a function of Al_2O_3 content. With regard to Y_2O_3 content, 2 mol% composites showed higher fracture toughness than corresponding 3 mol% composites. With regard to Al_2O_3 content, fracture toughness was found maximum also for the composites from 20 to 40 wt% Al_2O_3. This suggests: fracture toughness increased with increase in Al_2O_3 content at Al_2O_3 content from 0 to 20 wt% as a result of predominant increase in Young's modulus due to the increase in Al_2O_3 content, and reached maximum at Al_2O_3 content from 20 to 40 wt% as a result of further increase in Young's modulus balancing with the decrease in ZrO_2 content associated with increase in Al_2O_3 content[11], and finally decreased with increase in Al_2O_3 content at Al_2O_3 content higher than 60 wt% as a result of predominant decrease in the content of ZrO_2.

However, the mechanism that gave the ZrO_2-Al_2O_3 composites such high bending strength may not be explained only by the increase in fracture toughness mentioned above.

Fig. 3 shows the crack propagation behaviors for the composites of ZrO_2 of 2 mol% Y_2O_3 with Al_2O_3 content of 0, 20 and 80 wt%. At ZrO_2 alone, cracks propagated along the boundaries of fine ZrO_2 grains with small deflections. At Al_2O_3 content from 20 to 40 wt% which gave the highest fracture toughness, cracks pierced into the ZrO_2 grains markedly and deflected largely at the surface of Al_2O_3 grains. At Al_2O_3 content higher than 60 wt%, cracks propagated mainly along boundaries of large Al_2O_3 grains. This observation of crack propagation behaviors leads to the conclusion that, at Al_2O_3 content from 20 to 40 wt% where the highest fracture strength was obtained, pinning and deflection of crack by large Al_2O_3 grains and piercing into fine ZrO_2 grains of crack brought about the enhancement of fracture toughness and strength in addition to the effect of increasing Young's modulus.

(3) Crystal phase and microstructure

In the ZrO_2-Al_2O_3 composites, Al_2O_3 was all observed in the crystal form of trigonal α-Al_2O_3. ZrO_2 was found in the crystal forms of tetragonal, cubic and/or monoclinic. With regard to Y_2O_3 content, cubic ZrO_2 was not found for all of the 2 mol% composites indifferent of their Al_2O_3 content, but was found to increase up to 13 wt% with increase in Al_2O_3 content for the 3 mol% composites. Monoclinic ZrO_2 was not found for all of the 3 mol% composites. For the 2 mol% composites, monoclinic ZrO_2 was found at 2 wt% for ZrO_2 alone, but was found to decrease with increase in Al_2O_3 content.

Fig. 4 shows SEM photographs of the composites prepared with use of ZrO_2 containing Y_2O_3 of 2 mol%. Black and white particles represent Al_2O_3 and ZrO_2 grains, respectively. In the composites of Al_2O_3 content from 20 to 40 wt%, which showed the highest bending strength, large Al_2O_3 grains of about 0.7 μm in size were found to be dispersed uniformly and to be surrounded by small ZrO_2 grains of about 0.2 μm, and in addition, no crack and no flaw were found. The grain size of ZrO_2 was observed obviously to decrease with increase in Al_2O_3 content. Fig. 5 shows the mean grain sizes of ZrO_2 and Al_2O_3 measured from these SEM observations. Considering that the pre-sintering temperature was raised with increase in Al_2O_3 content, the addition of Al_2O_3 to ZrO_2 is concluded to have curbed the grain growth of ZrO_2 strongly. With regard to the Y_2O_3 content in ZrO_2, the grain size of ZrO_2 showed the tendency to become smaller for the 2 mol% composites than for the 3 mol% composites.

In discussing fracture strength of ZrO_2-Al_2O_3 composites, stress to initiate phase transformation of ZrO_2 from tetragonal to monoclinic should be considered as an important factor in addition to fracture toughness. Swain, who called this stress the critical stress, reported that fracture strength showed great dependence on the critical stress[12][13]. Based on this report, the increase in the critical stress due to the reduction in grain size of teragonal ZrO_2 is concluded to have played an important role to enhance the bending strength.

(4) Residual stress

Table IV shows residual stresses calculated from the results of X-ray diffraction of the composites prepared with use of ZrO_2 containing Y_2O_3 of 3 mol%. Phase stresses were found compressive for ZrO_2 and Al_2O_3 both:

about 80 MPa to ZrO_2 and about 200 MPa to Al_2O_3 at maximum. Macrostresses were found about 100 MPa compressive at maximum, which were supposed to have been introduced mainly by grinding process. It was considered that these stresses were not a predominant mechanism which led to the enhancement of bending strength. Microstresses which would be brought about by the thermal expansion mismatch between ZrO_2 and Al_2O_3, was found maximum for the composites from 20 to 40 wt% Al_2O_3 content, and showed tensile stress of about 50 MPa for ZrO_2 and compressive stress of about 100 MPa for Al_2O_3. These microstresses are averaged values within grains, and higher microstresses are expected in the vicinity of grain boundaries.

The crack propagation behaviors shown in Fig. 3 can be discussed also from the standpoint of microstresses. In the composites in which almost no microstresses were observed, cracks propagated along the grain boundaries of ZrO_2 and Al_2O_3. In the composites in which the Al_2O_3 content was from 20 to 40 wt% and the highest microstresses were observed, on the contrary, cracks propagated through inside ZrO_2 grains due to the tensile stress acting on ZrO_2 grains and propagated along the grain boundaries of Al_2O_3 with remarkable deflections due to the compressive stress acting on the Al_2O_3 grains.

4. Conclusion

To make clear the mechanism to give bending strength as high as about 3000 MPa, a number of ZrO_2-Al_2O_3 composites were prepared with varying Al_2O_3 content and using ZrO_2 raw powders containing different levels of Y_2O_3, and were examined in their mechanical properties, microstructure and residual stress. Results are as follows:

(1) The addition of 20 to 40 wt% Al_2O_3 to ZrO_2 gave both the maximum bending strength of 3000 MPa and the maximum fracture toughness of 7.5 MPa $m^{1/2}$.

(2) Residual microstresses were found about 50 MPa tensile for ZrO_2 grains and about 100 MPa compressive for Al_2O_3 grains. These residual microstresses led to the fracture mode change from inter-granular to trans-granular fracture at ZrO_2 grains and the large deflections at the Al_2O_3 grains.

(3) The Addition of Al_2O_3 to ZrO_2 curbed the grain growth of tetragonal ZrO_2 significantly.

(4) It is concluded that, the reduction of flaw size as fracture origins, the increase in fracture toughness and the rise of stress to initiate the stress-induced phase transformation of ZrO_2 from tetragonal to monoclinic could lead to the enhancement of bending strength of ZrO_2-Al_2O_3 composites.

References

1) A.G.Evans and R.M.Cannon, "Toughening of brittle solids by martensitic transformations", Acta Metall, 34, 5, 761-800(1986).

2) F.F.Lange, "Transformation toughening, Part 4 Fabrication, Fracture toughness and strength of Al_2O_3-ZrO_2 composites", J.Mater.Sci., 17, 1, 247-254(1982).

3) P.F.Becher, "Slow crack growth behavior in transformation-toughened Al_2O_3-ZrO_2 (Y_2O_3) ceramics", J.Am.Ceram.Soc., 66, 7, 485-488(1983).

4) K.Tsukuma, K.Ueda and M.Shimada, "Strength and fracture toughness of isostatically hot-pressed composites of Al_2O_3 and Y_2O_3-partially-

stabilized ZrO_2 ", J.Am.Ceram. Soc., 68, 1, c-4-c-5(1985).

5) M.Fukuhara, "Properties of (Y)ZrO_2-Al_2O_3 and (Y)ZrO_2-Al_2O_3-(Ti or Si)C composites", J.Am.Ceram.Soc., 72, 2, 236-242(1989).

6) M.Ishizuka, T.Sato, T.Endo and M.Shimada, "Sintering and mechanical properties of Yttria-doped tetragpnal ZrO_2 polycrystal/Mullite composites", J.Am.Ceram.Soc., 70, 11, c-342-c-346(1987).

7) A.Nakahira, Y.Fukushima and K.Niihara, "The Al_2O_3-SiC-ZrO_2 composites", J.Soc.Powder and Powder Metallurgy, 36, 6, 746-751(1989).

8) R.Shikata, Y.Urata, T.Shiono and T.Nishikawa, "Strengthening of Y-PSZ-Al_2O_3 composite ceramics", J.Soc.Powder and Powder Metallurgy,, 37, 2, 357-361(1990).

9) R.C.Garvie and P.S.Nicholson, "Phase analysis in Zirconia systems", J.Am.Ceram.Soc., 55, 6, 303-305(1972).

10) K.Tanaka, N.Mine, K.Suzuki, R.Shikata and T.Nishikawa, "Phase stress and bending strength of Zirconia-Alumina composites", Proc. of the 27th sympo. on X-ray studies on mechanical behavior of materials, 43-48(1990) Soc.Mater.Sci.Japan.

11) T.K.Gupta, F.F.Lange and J.H.Bechtold, "Effect of stress-induced phase transformation on the properties of polycrystalline zirconia containing metastable tetragonal phase", J.Mater.Sci., 13, 1464-1470(1978).

12) M.V.Swain, "Inelastic deformation of Mg-PSZ and its significance for strength－toughness relationship of zirconia toughened ceramics", Acta Metall, 33, 11, 2083-2091(1985).

13) M.V.Swain and L.R.F.Rose, "Strength limitation of transformation－toughened Zirconia alloys", J.Am.Ceram.Soc., 69, 7, 511-518(1986).

Table I. Characteristics of raw ZrO_2 powders.

No.	Specific surface area(m^2/g)	Crystallite size (nm)	Chemical composition (wt%)							
			ZrO_2	Y_2O_3	Al_2O_3	SiO_2	Fe_2O_3	TiO_2	Na_2O	Ig.loss
2 Y	20.3	21	95.9	3.6	0.005	0.004	0.004	0.004	0.005	0.4
3 Y	20.8	22	94.1	5.3	0.005	0.004	0.005	0.004	0.005	0.5

Table II. Characteristics of raw Al_2O_3 powder.

Crystal form	Specific surface area(m^2/g)	Mean particle size(μm)	Purity (%)	Impurity content (ppm)			
				Si	Mg	Fe	Na
α	4.4	0.54	99.99	25	3	11	3

Table III. X-ray conditions for stress measurement.

Method	Parallel beam method	
Characteristic X-ray	Cu-K_α	Cr-K_α
Diffraction plane	Al_2O_3(146)	ZrO_2(133)
Diffraction angle 2θ(deg)	136.30	152.35
Filter	Ni	V
Tube voltage (kV)	40	40
Tube current (mA)	40	30
Divergent angle (deg)	0.64	0.64
Irradiated area (mm^2 rectangle)	4×9.5	2×9.5
Scanning speed (deg/min)	1	1
Preset time (sec)	2	1
X-ray elastic constant $E/(1+\nu)$ (GPa)	343	129
Stress constant (MPa/deg)	-1201	-277

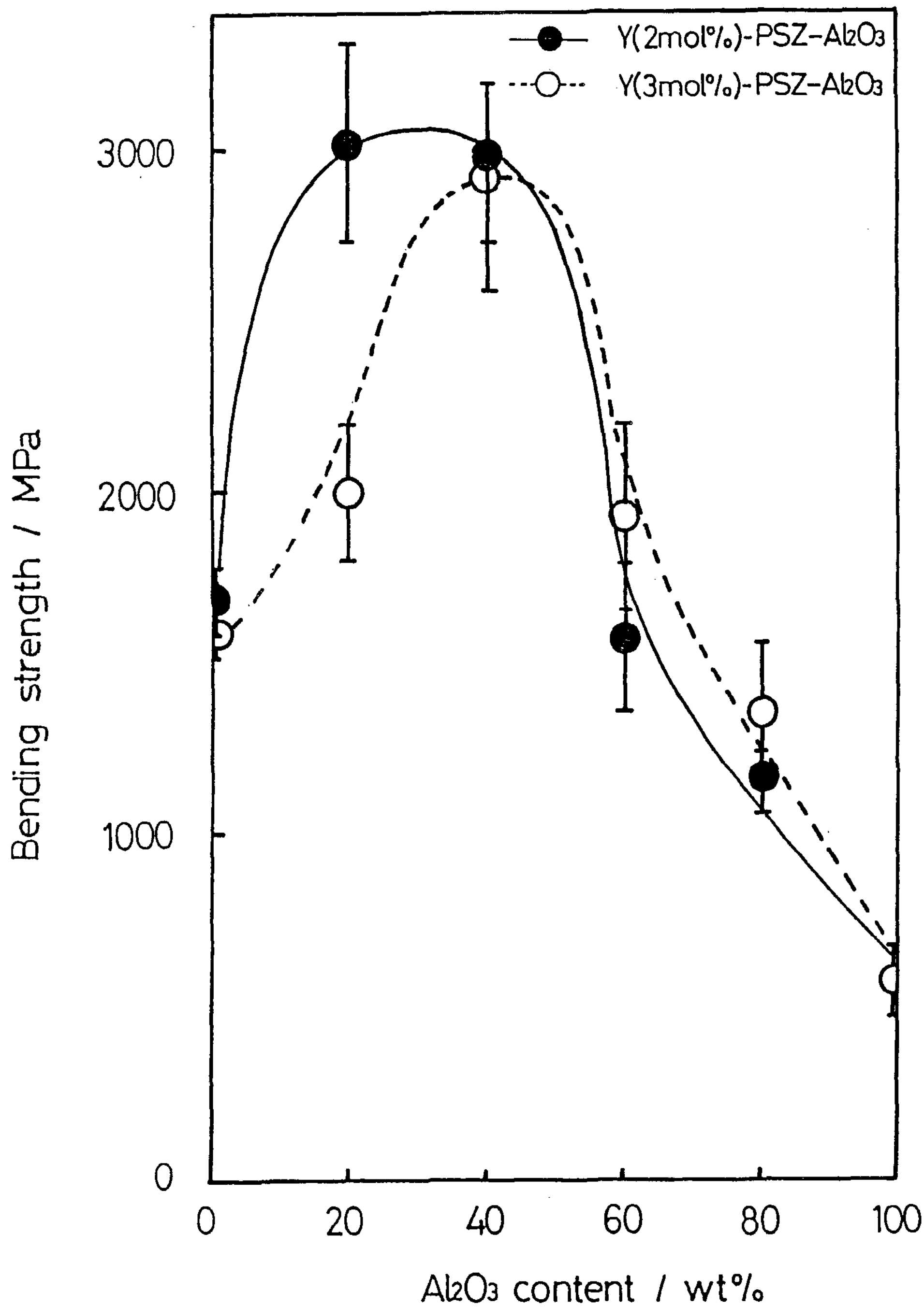

Fig. 1. Relation between Al_2O_3 content and bending strength of $ZrO_2-Al_2O_3$ composites.

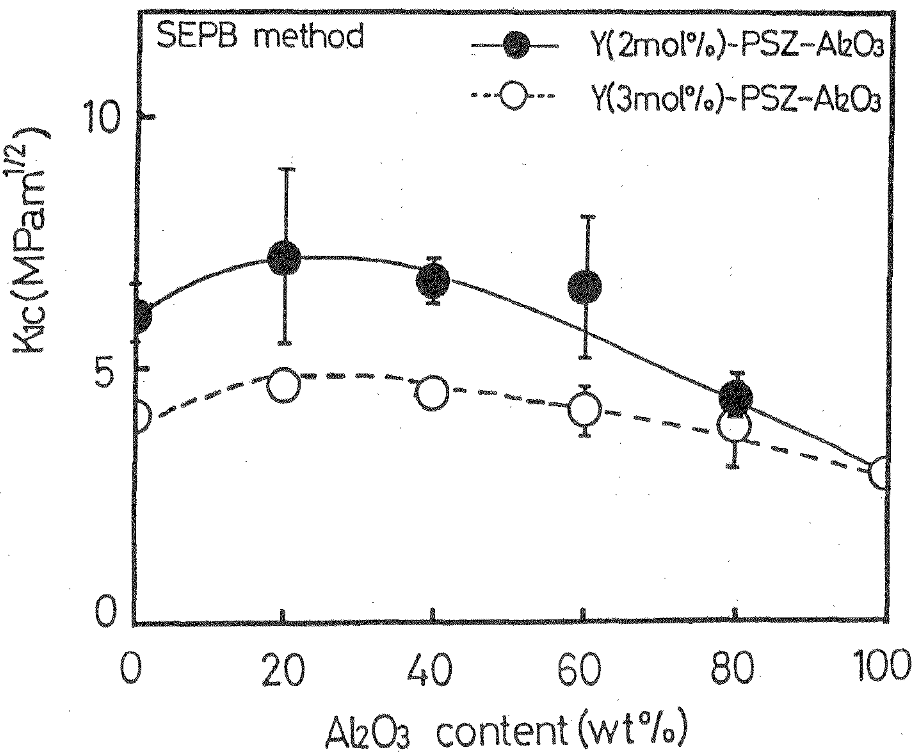

Fig. 2. Relation between Al_2O_3 content and fracture toughness by SEPB method.

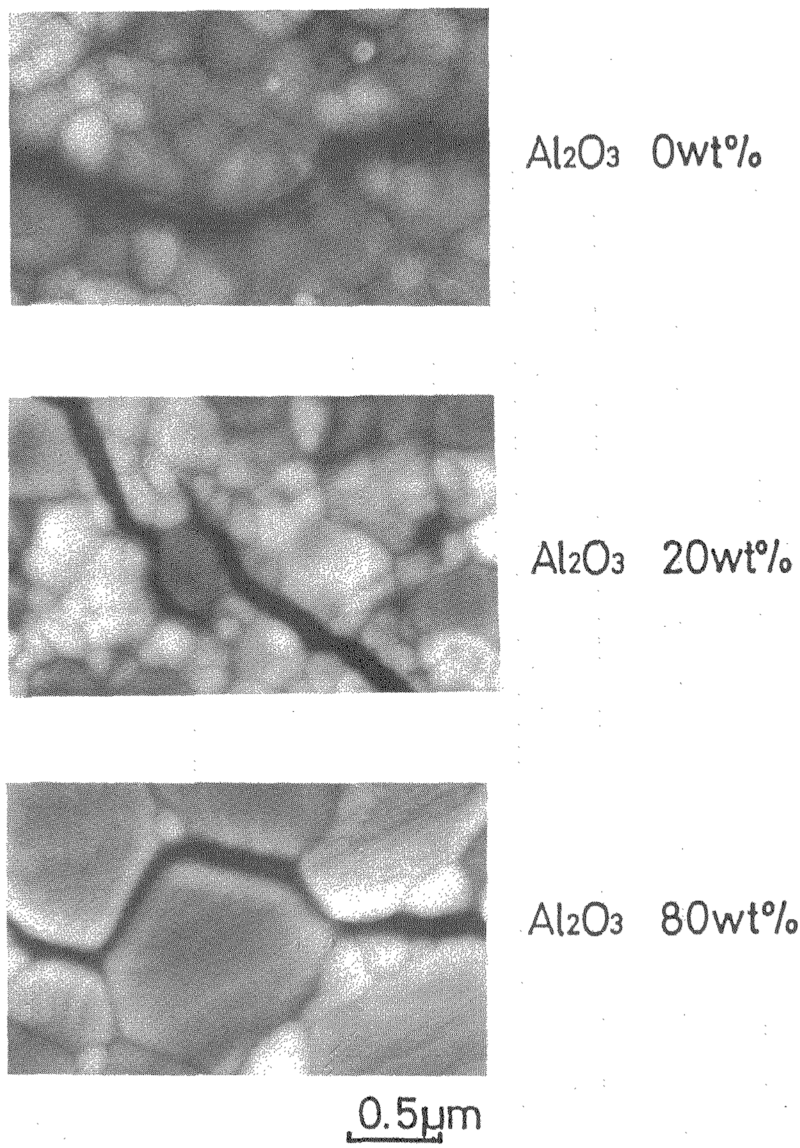

Fig. 3. Scanning electron micrographs of crack propagation behavior in ZrO_2 (2 mol% Y_2O_3)$-Al_2O_3$ composites by Vickers indentations.

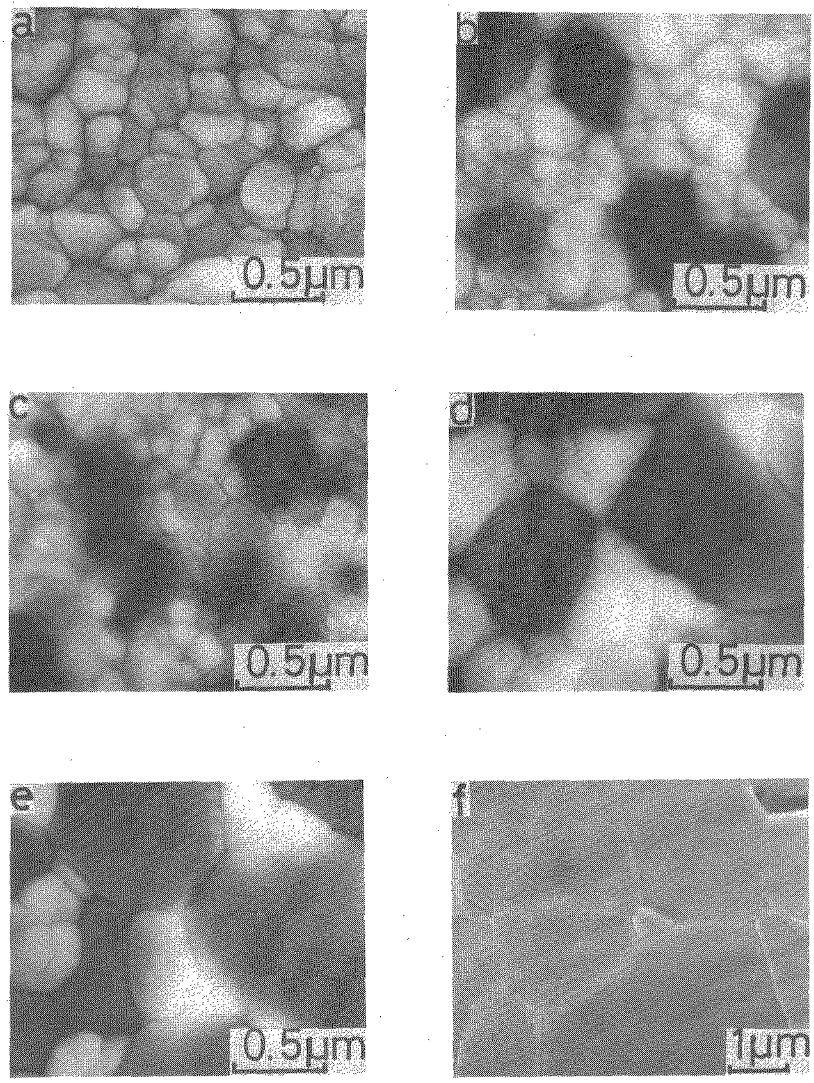

Fig. 4. Scanning electron micrographs of ZrO_2 (2 mol% Y_2O_3)$-Al_2O_3$ composites with Al_2O_3 additive of (a) 0wt%, (b) 20wt%, (c) 40wt%, (d) 60wt%, (e) 80wt% and (f) 100wt%.

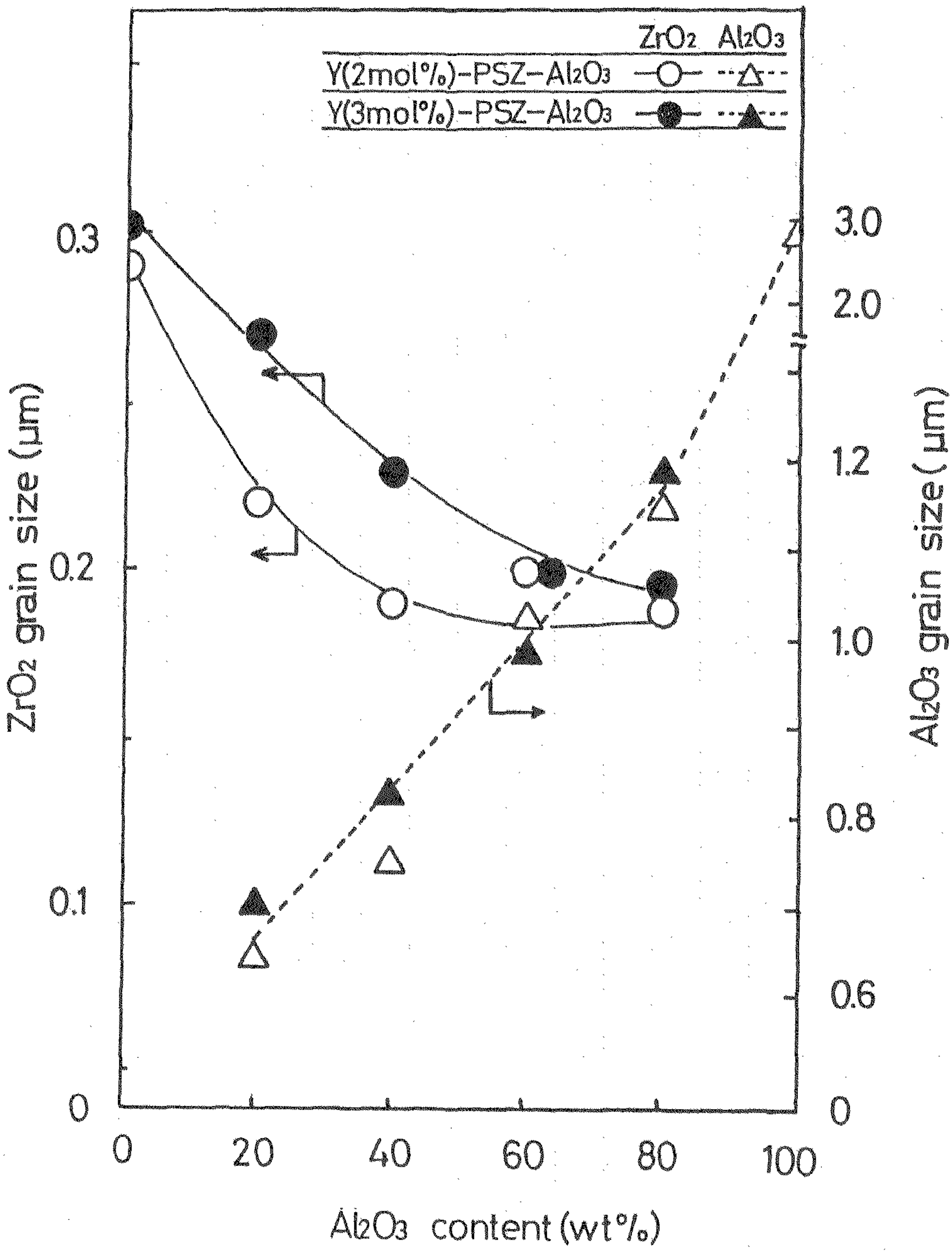

Fig. 5. Influence of the addition of Al_2O_3 on mean grain size of ZrO_2 and Al_2O_3 in $ZrO_2-Al_2O_3$ composites.

Table IV. Residual macro- and microstresses of ZrO_2 (3 mol% Y_2O_3)$-Al_2O_3$ composites.

Al_2O_3 content		Phase stress (MPa)		Macrostress (MPa)	Microstess (MPa)	
(wt%)	(vol%)	ZrO_2 (133)	Al_2O_3 (146)		ZrO_2	Al_2O_3
0	0	-33	-	-33	0	-
20	27.6	-78	-208	-114	36	-94
40	50.4	-49	-161	-105	56	-56
60	69.6	-31	-85	-69	38	-16
80	85.9	-4	-37	-32	28	-5
100	100	-	6	6	-	0